Effects of Optical Defocus on Refractive Development in Monkeys: Evidence for Local, Regionally Selective Mechanisms

Earl L. Smith III,[1,2] *Li-Fang Hung,*[1,2] *Juan Huang,*[1,2] *Terry L. Blasdel,*[3] *Tammy L. Humbird,*[3] *and Kurt H. Bockhorst*[4]

Purpose. To characterize the influence of optical defocus on ocular shape and the pattern of peripheral refraction in infant rhesus monkeys.

Methods. Starting at 3 weeks of age, eight infant monkeys were reared wearing −3 diopter (D) spectacle lenses over one eye that produced relative hyperopic defocus in the nasal field (NF) but allowed unrestricted vision in the temporal field (NF group). Six infants were reared with monocular −3 D lenses that produced relative hyperopic defocus across the entire field of view. Control data were obtained from 11 normal monkeys. Refractive development was assessed by streak retinoscopy performed along the pupillary axis and at eccentricities of 15°, 30°, and 45° along the vertical and horizontal meridians. Central axial dimensions and eye shape were assessed with magnetic resonance imaging.

Results. In response to full-field hyperopic defocus, the eye developed relative central axial myopia, became less oblate, and exhibited relative peripheral hyperopia in both the nasal and the temporal hemifields. Conversely, nasal-field hyperopic defocus produced relative myopia that was largely restricted to the nasal hemifield; these alterations in the patterns of peripheral refraction in the NF monkeys were associated with local, region-specific alterations in vitreous chamber depth in the treated hemiretina.

Conclusions. Optically imposed defocus can alter the shape and pattern of peripheral refraction in infant primates. Like those of form deprivation, the effects of optical defocus in primates are dominated by mechanisms that integrate visual signals in a spatially restricted manner and exert their influence in a regionally selective manner. (*Invest Ophthalmol Vis Sci.* 2010;51:3864–3873) DOI:10.1167/iovs.09-4969

In a wide range of species, from fish to primates, the growth and refractive status of the eye are regulated by visual feedback.[1] Moreover, evidence from birds and mammals indicate that the effects of vision on ocular growth and refractive development are mediated, in large part, by local retinal mechanisms (i.e., mechanisms that integrate visual signals in a spatially restricted manner and exert their influence selectively on the underlying sclera).[1,2] Understanding the operating characteristics of these local, vision-dependent mechanisms is important because peripheral vision, operating through these local mechanisms, could influence the eye's shape and, in particular, its axial length and central refractive development in a manner independent of visual signals from the central retina.

The local nature of ocular growth-regulating mechanisms was first demonstrated in chicks by showing that myopia could be produced in one portion of the eye while emmetropization proceeded normally in other parts. For example, in chicks, diffusers[3,4] or negative lenses[5] that cover only part of the visual field produce axial elongation and myopia that are restricted to the affected portion of the retina. It has subsequently been shown that hemiretinal form deprivation also alters ocular growth and refractive development in a regionally selective manner in tree shrews,[2] guinea pigs (McFadden SA. *IOVS* 2002;43:E-Abstract 189), and monkeys.[6] It is, however, not known whether optical defocus, a condition commonly experienced in everyday viewing, can produce localized changes in primate eyes. It is important to determine whether the effects of optical defocus are also mediated by local retinal mechanisms in primates because the effects of form deprivation and optical defocus on ocular growth appear to be mediated by different mechanisms.[7–9] In addition to providing insight into how peripheral vision may influence central refractive error, determining whether localized optical defocus can produce predictable changes in eye shape will provide a critical test in primates for the hypothesis that local retinal mechanisms regulate the shape of the eye to ensure the optimum focus across the retina.[4,10,11] Therefore, one goal of this study was to investigate the effects of hemiretinal optical defocus on ocular growth and the patterns of peripheral refraction in infant monkeys.

Because peripheral vision may influence central refractive development, it is important to know how optical defocus across the entire visual field influences ocular shape and the development of peripheral refractive error. In humans[12–17] and monkeys,[18] spherical-equivalent refractive errors can vary substantially with eccentricity. The patterns of peripheral refraction are correlated with central refractive error[12,14,19,20] and appears primarily to reflect the shape of the posterior globe.[18,21–23] For example, in humans, eyes with central axial myopia typically are less oblate/more prolate in shape and usually manifest relative hyperopia in the periphery.[24] The patterns of peripheral refraction have potentially significant clinical implications because the relative peripheral hyperopia found in myopic eyes has been implicated as a risk factor for myopia progression.[25–27] In particular, Hoogerheide et al.[25] reported that military recruits who exhibited relative peripheral hyperopia were more likely to develop myopia or exhibit

From the [1]College of Optometry and [3]Animal Care Operations, University of Houston, Houston, Texas; [2]Vision CRC, Sydney, Australia; and [4]University of Texas at Houston Medical School, Houston, Texas.

Supported by National Institutes of Health Grants EY-03611, EY-07551, and RR-17205 and funds from the Vision CRC and the UH Foundation.

Submitted for publication November 23, 2009; revised January 7 and February 10, 2010; accepted February 11, 2010.

Disclosure: **E.L. Smith III**, P; **L.-F. Hung**, None; **J. Huang**, None; **T.L. Blasdel**, None; **T.L. Humbird**, None; **K.H. Bockhorst**, None

Corresponding author: Earl L. Smith III, University of Houston, College of Optometry, 505 J. Davis Armistead Building, Houston, TX 77204-2020; smith@uh.edu.

myopia progression during pilot training than those who showed relative peripheral myopia. In support of the idea that peripheral refractive error are a risk factor for central refractive errors, evidence from laboratory animals indicates that peripheral vision can dominate central refractive development in primates[28,29] and, in particular, that optically imposed peripheral hyperopia can promote central axial myopia.[30]

Full-field form deprivation can alter ocular shape in monkeys. Specifically, in infant rhesus monkeys, full-field form deprivation produces central axial myopia and relative peripheral hyperopia. Relative peripheral hyperopia develops because as the central axial length increases, the eye becomes more prolate.[18] However, the effects of optical defocus may not be similar to those produced by form deprivation because, as mentioned, optical defocus and form deprivation are not mediated by identical mechanisms. In addition, the growth-altering effects of form deprivation and optical defocus may differ, at least quantitatively, as a function of eccentricity. Specifically, form deprivation, particularly the severe degrees of form deprivation typically used in studies of refractive development, would be expected to provide a strong signal for eye growth at all eccentricities. On the other hand, small to moderate degrees of optical defocus would likely produce proportionally smaller signals for ocular growth in the periphery than in the central retina because the spatial resolving capacity of the retina decreases with eccentricity. Thus, a second goal was to determine how optical defocus, specifically full-field hyperopic defocus, influences ocular shape and the patterns of peripheral refractive error.

Materials and Methods

Subjects

Data are presented for 25 infant rhesus monkeys (*Macaca mulatta*) obtained at 1 to 3 weeks of age and housed in our primate nursery, which was maintained on a 12-hour light/12-hour dark lighting cycle. Beginning at approximately 3 weeks of age (mean ± SD, 22 ± 3 days), eight monkeys were reared wearing goggles that held zero-powered lenses in front of the nontreated fellow eyes and spectacle lenses that produced −3 D of relative hyperopic defocus in the nasal visual fields of the treated eyes (nasal field [NF] subject group). We specifically chose to treat the nasal fields because this strategy was least disruptive to each animal's overall field of vision and, hence, was well tolerated by the animals. For example, with the nasal field treatment strategy, all parts of the field of view could be imaged simultaneously through either the zero-powered control lens or the zero-powered portion of the treatment lens. In contrast, with monocular temporal field treatment strategies, only the binocular field of view and the monocular temporal field ipsilateral to the control eye could be viewed simultaneously through zero-powered lenses. Moreover, the nasal field treatment strategy allowed us to compare our defocus data with previous results obtained from monkeys reared with nasal-field form deprivation.

Treatment lenses for the NF monkeys were commercially available wide-field, Franklin-type bifocal lenses that were edged to fit in the goggles so that the transition between the near and far segments of the lens was oriented vertically. When mounted in the goggles, the nasal and temporal segments of the lens had refracting powers of −3 D and 0 D, respectively, and the vertical transition between the two power zones was positioned approximately 1 mm to the temporal side of the center of the treated eye's entrance pupil while the eye was in primary gaze. Thus, the lenses allowed unrestricted vision in the temporal field and imposed −3 D defocus throughout the nasal visual hemifield. Given the position of the transition between the two power zones, it is also likely the foveal images in the treated eyes were at times degraded by the treatment lenses and that accommodation was controlled by the fellow eyes. The lenses were worn continuously until approximately 21 weeks of age (145 ± 11 days).

Six infants were reared with zero-powered lenses over the nontreated fellow eyes and −3 D single-vision spectacle lenses over the treated eyes (full field [FF] subject group). Treatment lenses imposed −3 D relative hyperopic defocus over the entire field of view (the extent of the vertical and horizontal fields of view for both the FF and the NF lenses were 87° and 80°, respectively) and were worn continuously from 22 ± 1 to 147 ± 5 days of age (see Ref. 31 for details of our nursery care and our goggle-rearing methods).

Control data for peripheral refraction was obtained from 11 normal animals (ages at measurement, 25.2 ± 4.9 and 162 ± 11 days); magnetic resonance imaging (MRI) was performed on six of the normal animals. Refraction data for all the normal monkeys have been reported.[18,32]

All the rearing and experimental procedures were reviewed and approved by the University of Houston's Institutional Animal Care and Use Committee and were in compliance with the ARVO Statement for the Use of Animals in Ophthalmic and Vision Research.

Ocular Biometry

The biometric measurements, which have been described in detail in previous publications,[31,32] were initially obtained at ages corresponding to the onset of lens wear and then at approximately 2-week intervals thereafter. Briefly, to obtain the ocular measurements, the animals were anesthetized (ketamine hydrochloride, 15–20 mg/kg; acepromazine maleate, 0.15–0.2 mg/kg) and cycloplegia was induced with 1% tropicamide. Spherical-equivalent refractive errors were determined by streak retinoscopy by two well-practiced investigators and averaged.[33] Central refraction was determined along the pupillary axis (i.e., the first Purkinje image produced by the retinoscope beam was observed in the center of the subject's entrance pupil). After measurements of central refraction, retinoscopy was performed at 15° intervals along either the vertical or the horizontal meridians to a maximum eccentricity of 45°. Because of time constraints, peripheral refraction was obtained along either the horizontal or the vertical meridians during a given session. Throughout this article, eccentricities for refractive errors are specified with respect to the visual field (e.g., temporal field measurements correspond to refractive errors for the nasal retina).

Ocular axial dimensions were measured by A-scan ultrasonography implemented with a 12-MHz transducer (OTI Scan 1000; OTI Ophthalmic Technologies, Inc, Toronto, ON, Canada). Intraocular distances were calculated from the average of 10 separate measurements using velocities of 1532 m/s, 1641 m/s, and 1532 m/s for the aqueous, lens, and vitreous, respectively. Corneal curvature was measured with a hand-held keratometer (Alcon Auto-keratometer; Alcon Systems Inc., St. Louis, MO) or a video topographer (EyeSys 2000; EyeSys Technologies Inc, Houston, TX).

Magnetic Resonance Image Acquisition

To assess the effects of the treatment regimens on the shape of the posterior globe, MRI was performed near the end of the lens-rearing period using a 7T horizontal bore scanner (Biospec USR70/30; Bruker, Karlsruhe, Germany). The details of our MRI procedures have been described previously.[18]

MRI was performed while the animals were anesthetized with 2% isoflurane gas anesthesia. After the initial tripilot scan to localize the position of the monkey's eyes, a localized shimming procedure (point resolved spectroscopy) was used to optimize magnetic field homogeneity. T_2-weighted anatomic images were obtained to enhance the contrast between the eye fluid and eye tissue (repetition time, 1000 ms; effective echo time, 169–179 ms). The spatial resolution of the axial images was 0.195 × 0.195 × 0.5 mm in the horizontal plane.

The acquired axial MR images were reconstructed using in-house software (MATLAB; MathWorks, Natick, MA), which identified the horizontal plane image that contained the approximate optical axis of the eye (defined as the perpendicular through the midpoint of the line connecting

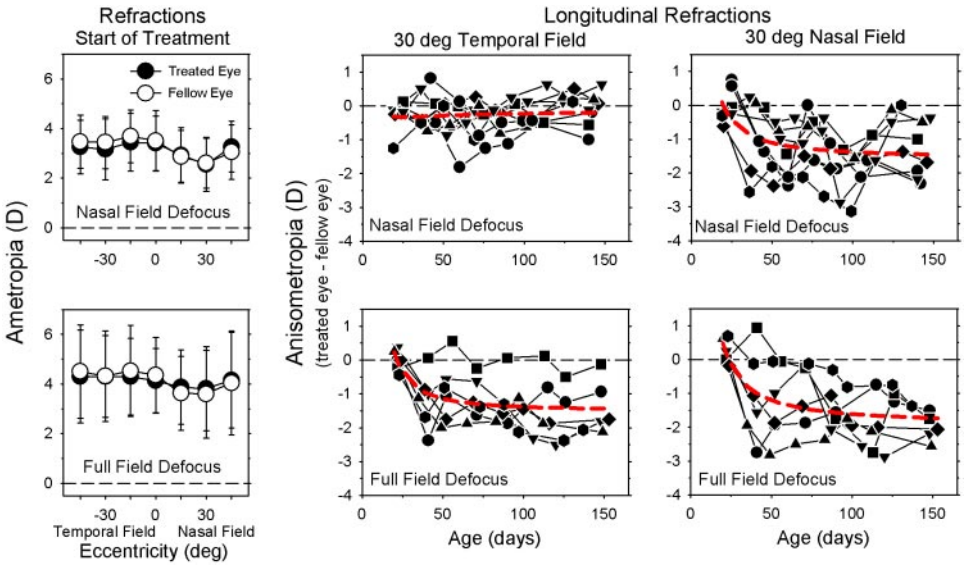

FIGURE 1. (*left*) Mean (±SD) spherical-equivalent refractive corrections obtained at the onset of the lens-rearing period plotted as a function of horizontal visual field eccentricity for the treated eyes (*filled circles*) and fellow eyes (*open symbols*) of the monkeys treated with nasal-field (*top*) and full-field −3 D lenses. *Middle*, *right*: interocular differences in refractive correction (treated eye − fellow eye) plotted as a function of age for the 30° temporal and 30° nasal field eccentricities for individual monkeys treated with nasal-field (*top*) and full-field −3 D lenses. *Red dashed lines*: second-order polynomials fitted to all the data plotted in a given panel.

the equatorial poles of the lens in the horizontal slice that showed the greatest lens thickness). The software interpolated between the axial image slices to produce a uniform resolution of 0.195 mm in the three-dimensional matrix, which, in terms of vitreous chamber depth, corresponded to a dioptric interval of approximately 1 D.

The intersection of the presumed optical axis and the posterior lens surface was considered to be the approximate position of the second nodal point and was used as the reference for specifying retinal eccentricities. The primary measure of interest was the vitreous chamber depth, defined as the distance between the approximate position of the second nodal point and the retina. Vitreous chamber depth in the horizontal meridian was determined as a function of eccentricity in 15° intervals to eccentricities of 45° using the approximate position of the posterior nodal point as a reference. As we have previously reported,[18] the vitreous chamber depths measured along the presumed optical axis by our MRI methods and A-scan ultrasonography were highly correlated ($r^2 = 0.89$; regression analysis of data from this study and from our previous study of form-deprived monkeys).[18] Our MRI measures were, on average, 0.07 mm shorter than our A-scan measures, and this difference was relatively constant over the range of vitreous chambers measured. The 95% limit of agreement for the two measures was ±0.45 mm, indicating that our MRI measures of vitreous chamber depth compared favorably with traditional A-scan measures.

Axial length and equatorial diameter were also measured in the horizontal MRI plane. Axial length was defined as the distance from the anterior corneal surface to the retina along the presumed optical axis. Equatorial diameter was defined as the greatest distance between the nasal and the temporal retinas measured along a line perpendicular to the presumed optical axis.

Statistical Analysis

Mixed-design, repeated-measures ANOVA (SuperANOVA; Abacus Concepts, Inc., Berkeley, CA) and multiple comparisons were used to determine whether there were differences in refractive error or vitreous chamber depth as a function of eccentricity or differences in the patterns of peripheral refraction between subject groups. For the repeated-measures analyses within subjects, probability values were adjusted with Geisser-Greenhouse correction to compensate for violations of the sphericity assumption.[34] For individual parameters, two-sample *t*-tests were used to compare mean values between subject groups, and paired *t*-tests were used for interocular or intraocular comparisons. The relationship between vitreous chamber depth and refractive error was analyzed using linear regression (Minitab Inc., State College, PA).

RESULTS

At the start of the lens-rearing period, the central refractive errors of the right eyes of treated monkeys were comparable to those of age-matched normal monkeys (normal monkeys, +3.42 ± 2.06 D; NF group, +3.40 ± 1.11 D; FF group, +4.13 ± 1.31 D). Specifically, there were no between-group differences in the right eyes in central refractive error (two-sample *t*-test, $T = -1.10$ to 0.03; $P = 0.30$–0.98) or vitreous chamber depth (two-sample *t*-test, $T = -0.02$ to 0.33; $P = 0.75$–0.99). Within a given experimental group, there were no systematic interocular differences in central refractive error (paired *t*-test, $T = -1.83$ to 0.51; $P = 0.11$–0.61) or vitreous chamber depth (paired *t*-test, $T = -0.56$ to 1.04; $P = 0.35$–0.59). In addition, before the treatment period, the patterns of peripheral refractive error in the two eyes of the treated monkeys were well matched ($F < 2.40$; $P > 0.05$) and similar to those found in normal monkeys ($F < 1.03$; $P > 0.05$). As illustrated in Figure 1 (left), the average peripheral refraction at the start of lens wear was relatively constant in the temporal field and similar to central refraction. However, as in normal monkeys,[32] refraction at the 15° and 30° nasal field eccentricities tended to be less hyperopic than did central refraction. Repeated-measures ANOVA indicated that these nasal-temporal asymmetries were significant in both eyes of the NF monkeys ($F > 3.92$; $P < 0.05$) and in the fellow eyes of the FF monkeys ($F = 7.20$; $P = 0.008$).

Shortly after the onset of lens wear, the nasal-field and full-field rearing strategies altered the interocular balance in peripheral refractive error. The middle and right plots in Figure 1 show the interocular differences in refractive error plotted as a function of age for individual treated monkeys for the 30° temporal and 30° nasal field eccentricities, respectively. For both the NF (top plots) and FF (lower plots) groups, the degree of relative myopia in the treated eyes tended to be larger in the nasal field, but the nasal-temporal disparity was greater in the NF-treated monkeys. It is also important to note that the time courses for the changes in anisometropia were rapid and comparable in both subject groups. For example, as illustrated by the second-order polynomial functions (red dashed lines) that were fit to the data, in both groups, the relative myopia in the nasal fields of their treated eyes was typically observed at the first or second measurement session after the onset of lens wear, and the degree of anisometropia was relatively stable

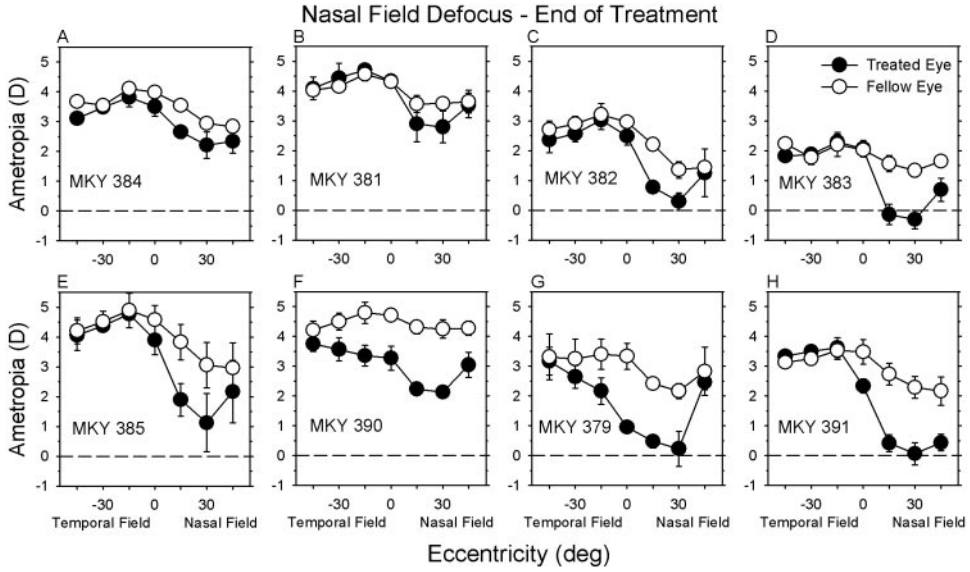

FIGURE 2. Spherical-equivalent refractive corrections plotted as a function of horizontal eccentricity for the treated eyes (*filled symbols*) and fellow eyes (*open symbols*) of individual monkeys treated with nasal-field −3 D lenses. The data points represent the mean ± SE for the final three measurement sessions of the treatment period.

after approximately 75 to 100 days of age. By inspection, the fitted functions provided a reasonable description of the overall data sets for both NF and FF monkeys. However, there was substantial intersubject variability toward the end of the treatment period, particularly in the NF group. For example, whereas two NF monkeys showed essentially no changes in anisometropia over the last three measurement sessions, two NF monkeys demonstrated increases in anisometropia over 0.5 D, and four NF monkeys exhibited decreases in the degree of anisometropia of >0.5 D. This variability may reflect the effects of transient periods of unrestricted vision in the treated nasal field produced by eye movements. We have previously found that even short periods of unrestricted vision can reduce the degree of myopia and substantially increase the intersubject variability in monkeys reared with optically imposed hyperopia.[35] However, the nonlinear manner in which signals that increase and decrease the rate of axial growth are integrated over time would at the same time reduce the effects of transient, eye movement–induced hyperopic defocus in the untreated temporal field.

At the end of the lens-rearing period, there were systematic differences in the patterns of peripheral refraction between the treated eyes and fellow eyes in both the NF and FF monkeys. The average spherical-equivalent refractive corrections (±SE) obtained during the last three measurement sessions of the lens-rearing period are plotted as a function of horizontal field eccentricity for NF- and FF-treated monkeys in Figures 2 and 3, respectively. All eight of the NF monkeys exhibited qualita-

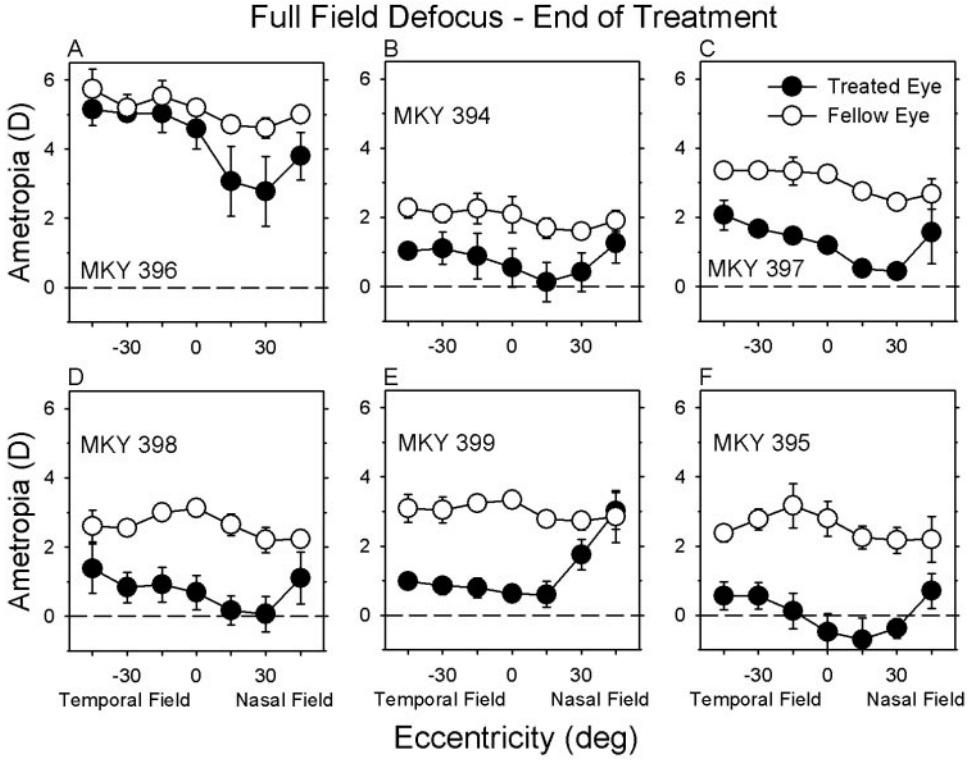

FIGURE 3. Spherical-equivalent refractive corrections plotted as a function of horizontal eccentricity for the treated eyes (*filled symbols*) and fellow eyes (*open symbols*) of individual monkeys treated with full-field −3 D lenses. The data points represent the mean ± SE for the final three measurement sessions of the treatment period.

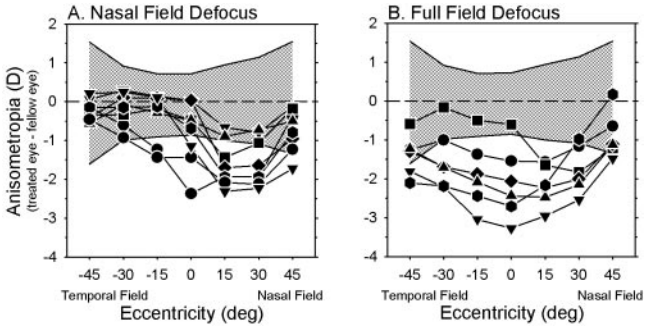

FIGURE 4. Interocular differences in refractive error (treated eye − fellow eye) obtained at the end of the lens-rearing period plotted as a function of horizontal eccentricity for individual monkeys that were reared with nasal-field (**A**) and full-field defocus (**B**). The cross-hatched area represents ±2 SD from the mean anisometropias for the normal animals obtained at 162 days of age (i.e., the normal monkeys were approximately 2 weeks older than the treated monkeys).

tively similar patterns of peripheral refraction. In their fellow eyes, the peripheral refraction in the nasal and temporal fields was similarly hyperopic or, more typically, less hyperopic than the central refraction, particularly in the nasal field in which the average refraction at the 15° and 30° eccentricities was approximately 1 D less hyperopic/more myopic than the central refraction. The absolute refractive errors in the temporal field of the treated eyes of the NF monkeys were similar to those in their fellow eyes. However, the absolute refractive errors in the nasal visual fields of the treated eyes were less hyperopic/more myopic than their fellow eyes in every NF animal.

The patterns of peripheral refraction in the fellow eyes of the FF monkeys were analogous to those found in the fellow eyes of the NF monkeys. However, with the exception of FF monkey 396 (Fig. 3A), which exhibited relative myopic changes that were primarily restricted to the nasal field, the treatment lenses consistently produced relative myopic changes over a larger portion of the horizontal field in the FF monkeys. In particular, peripheral refraction in the treated eyes of the FF monkeys was typically less hyperopic/more myopic than in fellow eyes at all the horizontal eccentricities examined.

Interocular comparisons emphasize the different patterns of peripheral refraction found in the fellow and treated eyes of the NF and FF monkeys at the end of the lens-rearing period. In Figure 4, the interocular differences in refractive error are plotted as a function of horizontal visual field eccentricity for individual NF (A) and FF (B) monkeys. For both groups of treated monkeys, the magnitude of anisometropia was greater than that observed in normal monkeys (NF monkeys: $F = 5.83$, $P = 0.002$; FF monkeys: $F = 3.58$, $P = 0.03$). Moreover, for both the NF and FF groups, refraction in the treated eyes was significantly more myopic than in the fellow eyes, and the degree of relative myopia varied with eccentricity (NF monkeys: $F = 8.53$, $P = 0.001$; FF monkeys: $F = 5.50$, $P = 0.05$). For seven of the eight NF monkeys, the greatest interocular differences in refractive error were observed at the 15° or 30° nasal field eccentricities, and for six of the eight NF monkeys, these nasal field interocular differences fell outside 2 SD of the mean interocular differences for the normal monkeys (shaded area). On the other hand, the degree of anisometropia was within 2 SD of the normal average at the 30° and 45° temporal field eccentricities for all the NF monkeys and at the 15° temporal field eccentricity for six of the eight NF monkeys.

Treated eyes of the FF monkeys were, on average, more myopic than their fellow eyes at all eccentricities. As in the NF monkeys, the degree of relative myopia in the treated eyes of the FF monkeys varied with eccentricity. In the FF monkeys, the greatest degree of myopic anisometropia was observed along the pupillary axis or at the 15° nasal field eccentricity. For five of the six FF monkeys, the anisometropias for the central 30° (i.e., nasal 15°, 0°, and temporal 15°) were outside 2 SD from the normal averages. Similarly, the anisometropias for five of the six FF monkeys were outside the 2 SD limits of the normal average at the 30° eccentricities in both the nasal and temporal visual fields. In essence, five of the six FF monkeys exhibited relative peripheral hyperopia in both the nasal and the temporal hemifields of the treated eyes (i.e., the degree of myopic anisometropia decreased with increasing horizontal field eccentricity).

In addition to the interocular differences in the horizontal peripheral refraction between the treated and fellow eyes of the NF and FF monkeys, there were eccentricity-dependent, between-group differences in the degree of anisometropia and in the patterns of peripheral refraction for the treated eyes. The left column of Figure 5 illustrates the average (±SE) refractive corrections obtained at ages corresponding to the end of the

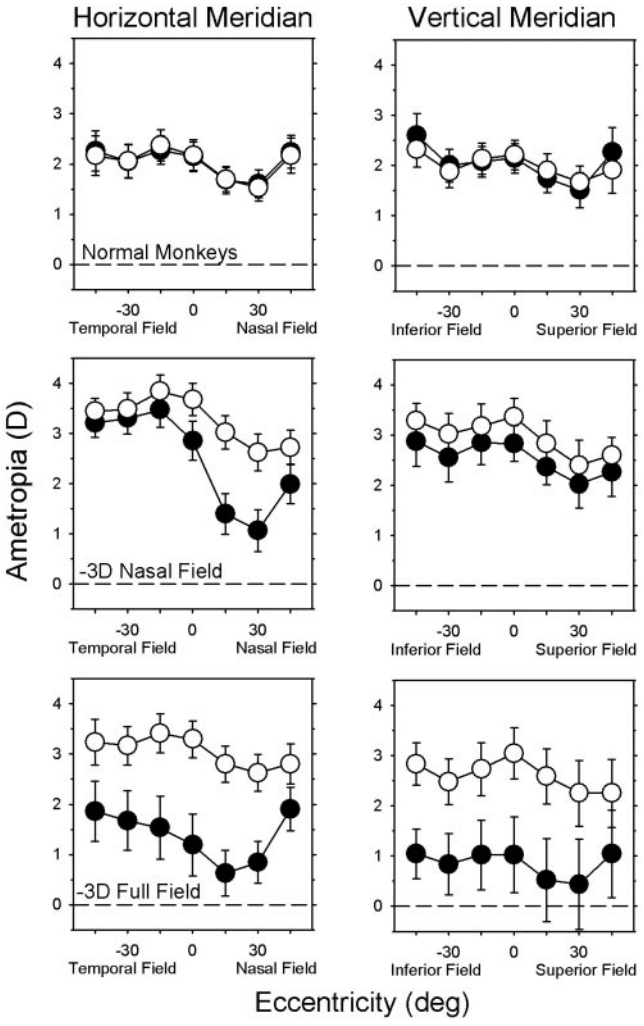

FIGURE 5. Mean (±SE) spherical-equivalent refractive corrections (treated or right eyes, *filled symbols*; fellow or left eyes, *open symbols*) plotted as function of horizontal (*left*) and vertical (*top*) visual field eccentricities for the normal, NF (*middle*), and FF monkeys (*bottom*). For the NF and FF monkeys, the data were obtained at the end of the lens-rearing period (145 ± 11 and 147 ± 5 days, respectively); the normal monkey data were obtained at 162 ± 11 days of age.

treatment period along the horizontal meridian for the normal (top), NF (middle), and FF monkeys (bottom) (treated or right eyes, filled symbols; fellow or left eyes, open symbols). In the normal monkeys, there was a systematic reduction in the degree of hyperopia at all eccentricities between the ages corresponding to the onset and end of the lens-rearing period for the treated monkeys (i.e., emmetropization occurred), and, as expected, the patterns of peripheral refraction for the left and right eyes of the normal monkeys changed very little over time and were well matched at the end of the observation period ($F = 0.23$; $P = 0.81$). The central refraction of the fellow eyes of the NF and FF monkeys were slightly more hyperopic than those for the control eyes (NF monkeys: $T = -3.07$, $P = 0.007$; FF monkeys: $T = -1.79$, $P = 0.11$); however, there were no systematic differences in the magnitude and pattern of peripheral refraction between the fellow eyes of the NF and FF monkeys ($F = 0.93$; $P = 0.41$). On the other hand, intergroup comparisons showed that there were significant differences in the pattern of horizontal peripheral refraction between the treated eyes of the NF and FF monkeys ($F = 3.65$, $P = 0.04$). In particular, for the NF monkeys, there were obvious nasal-temporal asymmetries in peripheral refraction along the horizontal meridian ($F = 24.47$; $P = 0.0001$). Although the absolute treated-eye refractive errors for the FF monkeys were more myopic than those for the NF monkeys at all eccentricities, there were no significant nasal-temporal asymmetries in the pattern of peripheral refraction in the treated eyes of the FF monkeys ($F = 3.73$; $P = 0.09$). As a consequence of the different patterns of peripheral refraction in the treated eyes, there were significant eccentricity-dependent differences in the degree of anisometropia between the NF and FF monkeys ($F = 11.38$; $P = 0.0001$). Specifically, the myopic anisometropias for the three nasal field eccentricities were similar in the NF and FF monkeys ($T = 0.52–1.86$; $P = 0.09–0.61$); however, the NF monkeys exhibited significantly smaller amounts of myopic anisometropia centrally and at all three temporal field eccentricities ($T = 2.69–4.89$; $P = 0.003–0.03$).

Comparisons of peripheral refraction along the horizontal and vertical meridians also revealed substantial differences in the pattern of refractive changes in the treated eyes of the NF and FF monkeys. The right column of Figure 5 shows the average (±SE) refractive corrections obtained near the end of the treatment period along the vertical meridian for the three subject groups. The patterns of refractive changes produced by the full-field treatment lenses in the vertical and horizontal meridians were similar (bottom plots). As in the horizontal meridian, the treated eyes of the FF monkeys were significantly more myopic than their fellow eyes at all eccentricities along the vertical meridian ($F = 34.90$; $P = 0.002$). More importantly, the degree of relative myopia in the treated eyes of the FF monkeys was the same along both the vertical and the horizontal meridians ($F = 0.001$; $P = 0.98$). On the other hand, the lens-induced changes in refraction were very different in the horizontal and vertical meridians of the NF monkeys. There was a trend for the treated eyes of the NF monkeys to be less hyperopic/more myopic than their fellow eyes at all eccentricities along the vertical meridian ($F = 3.35$; $P = 0.11$); however, in contrast to the obvious nasal-temporal asymmetries in the horizontal meridian, the treated eyes of the NF monkeys exhibited approximately the same small degree of relative myopia at all eccentricities in the vertical meridian ($F = 0.17$; $P = 0.87$).

The refractive changes observed in the treated monkeys were axial. For example, although the NF monkeys had significant degrees of anisometropia in the nasal field and the FF monkeys had significant degrees of anisometropia at all horizontal field eccentricities, keratometry showed no interocular differences in central corneal power (spherical equivalent power: NF monkeys, +55.95 ± 1.85 vs. +55.89 ± 1.84 D; $T = 0.37$; $P = 0.72$; FF monkeys, +55.10 ± 1.34 vs. +55.21 ± 1.55 D; $T = -0.41$; $P = 0.70$), and A-scan ultrasonography revealed no interocular differences in anterior chamber depth (NF monkeys: 3.18 ± 0.15 vs. 3.18 ± 0.16 mm, $T = -0.23$, $P = 0.82$; FF monkeys: 3.14 ± 0.17 vs. 3.13 ± 0.15 mm, $T = 0.20$, $P = 0.85$), or crystalline lens thickness (NF monkeys: 3.67 ± 0.10 vs. 3.68 ± 0.08 mm, $T = -0.51$, $P = 0.62$; FF monkeys: 3.61 ± 0.11 vs. 3.65 ± 0.11 mm, $T = -1.25$, $P = 0.27$). However, the FF monkeys exhibited significantly longer axial vitreous chamber depths (FF monkeys: 10.43 ± 0.63 vs. 10.00 ± 0.56 mm, $T = 5.59$, $P = 0.003$; NF monkeys: 9.71 ± 0.45 vs. 9.68 ± 0.33 mm, $T = 0.44$, $P = 0.68$).

The MR images also revealed interocular differences in vitreous chamber depth in the treated monkeys and, more importantly, changes in the shapes of the posterior globe that mirrored the alterations in the patterns of peripheral refraction in the treated eyes of the NF and FF monkeys. Figure 6 illustrates horizontal MR images obtained at the end of the lens-rearing period for the treated and fellow eyes of representative NF (top two rows) and FF monkeys (bottom two rows). Although the alterations in eye shape for the NF and FF monkeys were not as obvious as those we have previously reported for nasal field and full field form-deprived monkeys,[6,18] the overlapped images in the right panels emphasize the nature of the changes in eye shape. Specifically, for both the NF and the FF monkeys, the anterior segment image outlines for the fellow and treated eyes superimpose, but the there are eccentricity-dependent differences in the depth of the vitreous chamber for both the NF and the FF monkeys.

The differences in vitreous chamber depth obtained from the MRIs are quantified in Figure 7, which shows the average (±SE) vitreous chamber depths plotted as a function of horizontal eccentricity for all three subject groups (treated or right eyes, filled symbols; fellow or left eyes, open symbols). As observed previously, vitreous chamber depth was consistently greater on the temporal side of the globe in the control and fellow eyes.[18] The vitreous chambers of the fellow eyes of the FF and NF monkeys were generally shorter than those of the normal monkeys, which probably contributed to the more hyperopic refractive errors observed in the fellow eyes of the treated monkeys. In contrast to the normal animals, which showed no systematic interocular differences in vitreous chamber depth (right column; $F = 0.81$; $P = 0.47$), the NF and FF monkeys exhibited significant interocular differences in vitreous chamber depth that varied with eccentricity ($F > 8.83$; $P < 0.02$). For the NF monkeys, the relative increases in vitreous chamber depth were restricted to the temporal half of the globe ($F = 119.58$; $P = 0.0001$); no interocular differences in vitreous chamber depth were observed for the nasal retinas (i.e., temporal fields) of the NF monkeys ($F = 0.14$; $P = 0.50$). The increases in vitreous chamber depth of the treated eyes were greater in magnitude in the FF than in the NF monkeys, and these between-group differences varied with eccentricity ($F = 6.80$; $P = 0.0001$). The relative interocular differences in vitreous chamber depth in the FF monkeys were observed at all eccentricities, though they were smallest at the 45° eccentricities, indicating that the treated eyes had become more prolate/less oblate than their fellow eyes.

Comparisons of the axial lengths (corneal to vitreoretinal interface along the presumed optical axis) and equatorial diameters (greatest diameter measured perpendicularly to the optical axis in the horizontal plane) obtained from the MRI scans indicated that the equatorial diameters were greater than the axial lengths in all eyes; in other words, all the eyes were actually oblate ($T = -4.12$ to -11.5; $P = 0.0001–0.009$). The treated eyes of the FF monkeys showed significant interocular

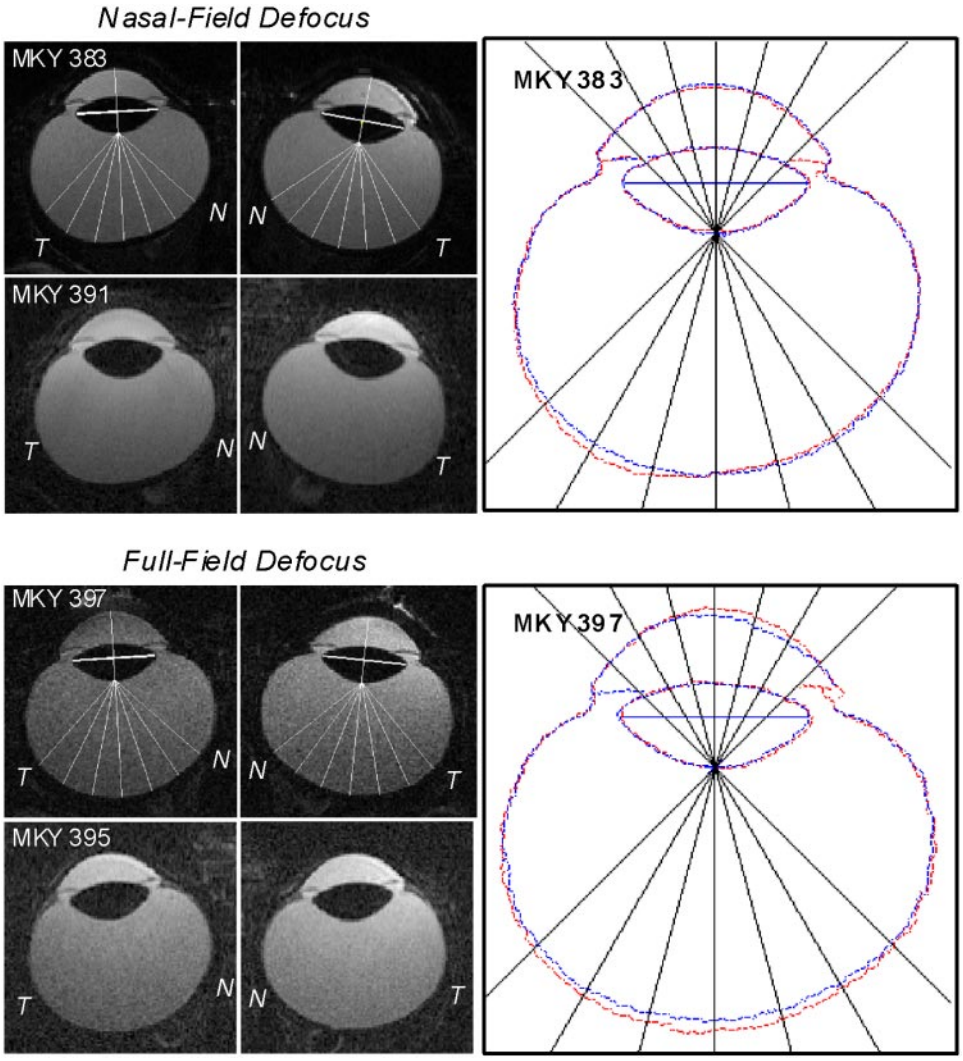

FIGURE 6. Magnetic resonance images for the horizontal plane obtained at the end of the lens-rearing period for the treated eyes (*left*) and fellow eyes (*right*) of representative NF (*top two rows*; *left, middle*) and FF (*bottom two rows*; *left*, *middle*) monkeys. The nasal and temporal aspects of the images are labeled *N* and *T*, respectively. Vitreous chamber depths were measured from the intersection of the presumed optical axis and the posterior lens surface to the vitreous-retina interface as a function of eccentricity from 45° nasally to 45° temporally in 15° intervals along the horizontal meridian. *Right*: outlines for the treated (*red*) and fellow (*blue*) eyes of the top NF (MKY 383) and FF monkeys (MKY 397) have been superimposed after rotating the fellow eye images around the optic axes so that the nasal retinas are shown to the right for both eyes. The superimposed images were aligned using the lines that connected the equatorial poles of the crystalline lenses as a reference (*thick white lines* shown in the treated and fellow eye images in the *left* and *middle* columns).

increases in axial length ($T = 3.93$; $P = 0.01$) and equatorial diameter ($T = 4.06$; $P = 0.01$). Average interocular increases in axial length were greater than those for the equatorial diameters (0.45 vs. 0.31 mm), indicating that the eyes had become less oblate; however, these differences between the increases in axial length and equatorial diameter did not reach statistical significance ($T = 1.16$; $P = 0.30$).

Regression analysis demonstrated that the interocular differences in peripheral refraction were caused mainly by interocular differences in vitreous chamber depth. In Figure 8, the interocular differences in peripheral refractive error along the horizontal meridian are plotted as a function of the interocular differences in vitreous chamber depth for all three subject groups. For the combined data set, the local interocular differences in refractive error were significantly correlated with the local interocular differences in vitreous chamber depth, with an r^2 value of 0.49 ($P < 0.0001$).

DISCUSSION

The interocular and between-group comparisons demonstrate that hyperopic defocus optically imposed across either the

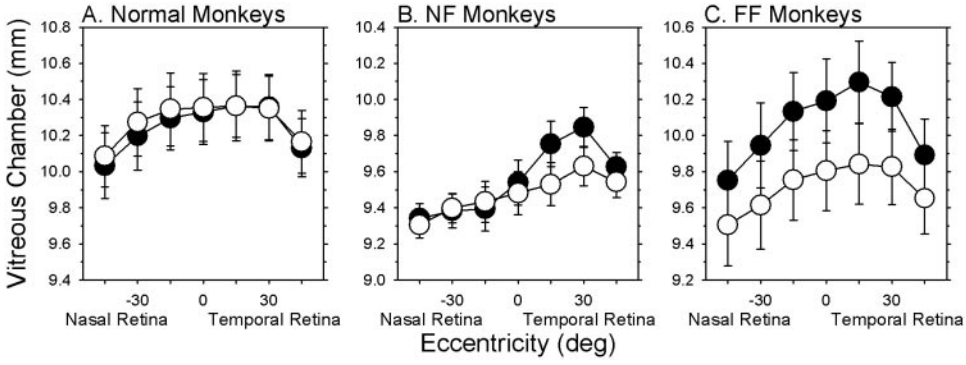

FIGURE 7. Mean (±SE) vitreous chamber depth (treated or right eyes, *filled symbols*; fellow or left eyes, *open symbols*) plotted as a function of horizontal retinal eccentricity for the normal (**A**), NF (**B**), and FF monkeys (**C**). The data were obtained at ages near the end of the lens-rearing period for the treated monkeys.

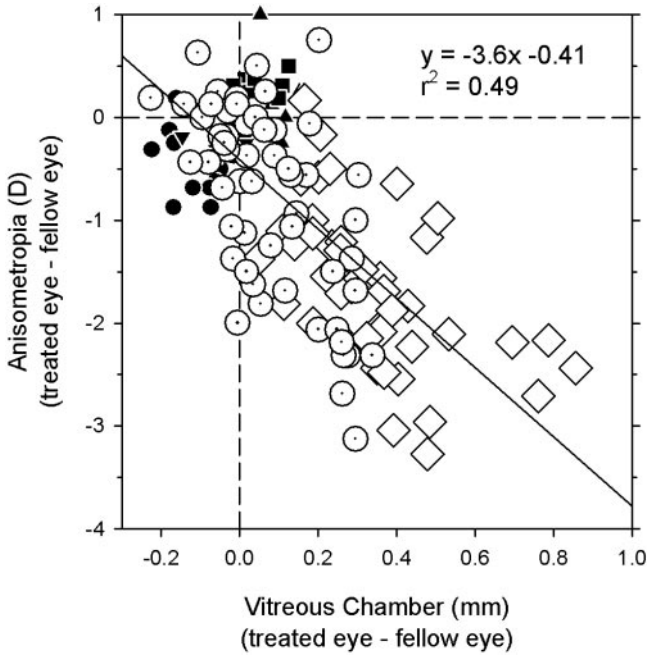

FIGURE 8. Interocular differences in refractive error obtained at ages corresponding to the end of the lens-rearing period plotted as a function of interocular differences in vitreous chamber depth (treated or right eye − fellow or left eye). Data are shown for the normal (*filled symbols*), NF, (*open dotted circles*), and FF (*open diamonds*) monkeys for all eccentricities along the horizontal meridian. *Solid line*: best-fitting regression line.

entire visual field or only across the nasal visual field can produce alterations in ocular shape and the pattern of peripheral refraction. With full-field hyperopic defocus, the increases in vitreous chamber depth along the horizontal meridian were greatest in the central and the near temporal retina (the posterior globe became less oblate/more prolate). Similarly, the myopic refractive changes produced by full-field defocus were greatest near the central retina and decreased with eccentricity (treated eyes exhibited relative peripheral hyperopia). On the other hand, nasal field hyperopic defocus produced increases in vitreous chamber depth and relative myopia that were largely restricted to the treated hemifield.

The differences in ocular shape and the patterns of peripheral refraction produced by the FF and NF treatment regimens support the idea that in primates the effects of optical defocus are mediated by local, vision-dependent mechanisms that act in a regionally selective manner. With FF defocus, the alterations in refractive error were similar in magnitude in all hemifields, presumably reflecting the fact that the treatment lenses imposed relative hyperopic defocus across the entire field of view. In this respect, the pattern of peripheral refraction in the FF monkeys demonstrates that optical defocus can alter refractive development in all hemifields. Thus, in the NF monkeys, the nasal-temporal asymmetries in refractive error along the horizontal meridian and the substantial differences in the pattern of refractive-error changes between the vertical and horizontal meridians do not reflect an inability of the nasal, superior, or inferior hemiretinas to change in response to optically imposed defocus. Instead, they emphasize that the shape of the eye can be altered in a spatially localized manner to optimize refractive error across the visual field. The ability of the eye to compensate for locally imposed optical errors also argues against the idea that signals associated with accommodative tonus or any other presumably global-acting mechanisms (e.g., intraocular pressure) play a primary role in the regulation of refractive development associated with emmetropization.[5,6]

The patterns of refractive changes produced by FF and NF defocus in infant monkeys are qualitatively similar to those produced by full-field and nasal-field form deprivation, respectively.[6,18] Thus, in monkeys the effects of both optical defocus and form deprivation are mediated by mechanisms, presumably located in the retina,[36] that sample the retinal image in a regionally selective manner and exert their influence on ocular growth locally. Although there is evidence that the effects of form deprivation and optical defocus are mediated by different mechanisms,[7–9] the parallels between the results obtained with defocus and form deprivation suggest that there are elements that are common to both mechanisms; possibly they share a common final pathway.

There were also quantitative similarities in the changes in vitreous chamber depth and the degree of peripheral hyperopia produced by FF form deprivation versus FF defocus. Figures 9A and 9B compare, respectively, the patterns of relative peripheral refractive error and the alterations in vitreous chamber depth produced by FF form deprivation (gray diamonds) and FF optical defocus (filled circles). Because at a given eccentricity the degree of relative peripheral hyperopia increases systematically with the degree of central myopia, the relative peripheral refractive errors were calculated for a theoretical form-deprived eye with a central refractive error equal to that of the average central refractive error of the FF defocus monkeys. Specifically, the relative peripheral refractive errors for an equivalent form-deprived eye were calculated from the relative peripheral refractive error versus central refractive error functions generated in our previous study of FF form-deprived monkeys (see Figure 4 in Ref. 18). Similarly, the relative interocular differences in vitreous chamber depth were calculated for a theoretical monocularly form-deprived monkey that had a central anisometropia equal to that of the average FF defocus monkeys. The peripheral refractive error function for the FF defocus monkeys in Figure 9A represents the treated-eye data from Figure 5 normalized to the central ametropia; the relative vitreous chamber depth data for the FF defocus monkeys represent the normalized intraocular differences of the average vitreous chamber depths shown in Figure 7.

Because the functional consequences of optical defocus are presumably greatest in the central retina and decrease with eccentricity, one might expect optical defocus to preferentially promote central axial elongation and result in an eye shape that is more prolate than does form deprivation. In other words, one might expect to find a higher amount of relative peripheral hyperopia with full-field defocus. However, as illustrated in

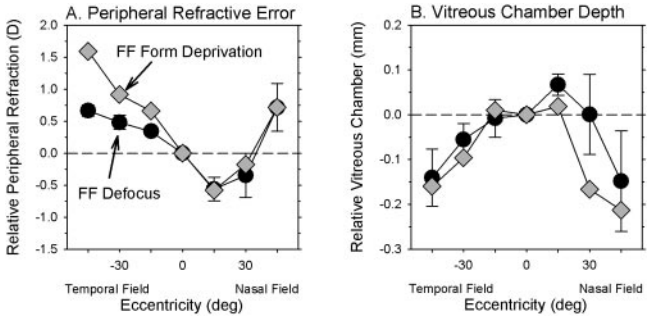

FIGURE 9. Relative peripheral refractive error (**A**) and relative interocular differences in vitreous chamber depth (**B**) plotted as a function of eccentricity for monkeys reared with full-field form deprivation (*gray diamonds*) or optical defocus (*filled circles*, mean ± SE). The refractive error and vitreous chamber data for FF form deprivation were calculated for a theoretical form-deprived eye that had a central refractive error equal to that of the average FF defocus monkey.

Figure 9, there is generally good agreement between the defocus and form deprivation data. For the temporal field, the relative refractive error data for the FF defocus monkeys appear to asymptote whereas the degree of relative peripheral hyperopia in the form-deprived monkeys continues to increase with eccentricity; however, the FF defocus data fall within the 95% confidence limits for the FF form deprivation data at all eccentricities for both the refractive error and the vitreous chamber depth plots. The key point is that when comparable degrees of central axial myopia are considered, both defocus and form deprivation produce comparable changes in vitreous chamber shape and the pattern of peripheral refractive error, which suggests that the nature of shape changes produced by form deprivation and optical defocus are influenced by the same factors.

There were, however, some differences in the refractive changes produced by defocus and form deprivation. Although the changes in peripheral refraction produced by optical defocus and form deprivation[18] were observed very early in the course of treatment, the magnitude of the myopic changes produced by full-field and nasal-field form deprivation generally increased in magnitude throughout the treatment period.[6,18] On the other hand, the effects of optical defocus reached their maximum well before the end of the treatment period. This difference probably reflects the fact that form deprivation provides a strong signal for growth throughout the rearing period and, in essence, represents unregulated, "open-loop" growth. On the other hand, with optical defocus, the error signal decreases as the eye compensates for the imposed defocus. In other words, the changes in the animals subjected to optically imposed defocus represent regulated lens compensation rather than uncontrolled growth.

In both marmosets and macaques, full-field, optically imposed hyperopic defocus can produce central axial myopia and peripheral hyperopic defocus. The pattern of peripheral refraction in our FF monkeys was different, however, from that reported for lens-reared marmosets. In marmosets reared with negative lenses in front of one eye and positive lenses in front of the fellow eye, interocular comparisons showed that the more myopic eyes (the eyes treated with negative lenses) exhibited relative peripheral hyperopia in the temporal visual field but not in the nasal visual field.[37] The nasal-temporal asymmetries observed in myopic marmoset eyes came about because the increases in vitreous chamber were primarily restricted to the nasal field/temporal retina. The average data for our FF monkeys showed that the myopic changes were also greater in the near nasal field than in the near temporal field. However, in our macaques, the changes were obvious in both hemifields. The presence of the optic disc may constrain vision-dependent changes in the nasal retina. In normal monkeys, the vitreous chamber depth is typically greater in the temporal than in the nasal retina, and monkeys treated with FF form deprivation, like our FF defocus monkeys, exhibit greater increases in vitreous chamber depth in the near temporal than in the near nasal retinas. Some of this bias may occur because the pupillary axis normally intersects the retina nasal to the fovea. As a consequence, the "central retinal" reference for our peripheral refractive error measures was displaced nasally relative to the visual axis by approximately 2° to 3°.[38] However, there are also well-documented nasal-temporal differences in the density of many retinal neurons along the horizontal meridian. Possibly the strength of growth signals or those that stop growth vary with the density of some critical population of retinal neurons. In this respect, neuron densities are generally higher in the nasal than the temporal retina.[39]

Our results in infant NF macaques are qualitatively similar to the refractive changes produced by locally imposed optical defocus or form deprivation in chickens,[3–5] tree shrews,[40] and guinea pigs (McFadden SA. *IOVS* 2002;43:ARVO E-Abstract 189). In particular, in all these species, restricting the visual signals for growth to one hemifield produces relative myopic changes that are largely restricted to the treated hemifield. These parallels across species represent another observation that shows the operational properties of the vision-dependent mechanisms that regulate refractive development have been conserved during evolution and, even though vision in monkeys is dominated by foveal vision, the prominence of local retinal mechanisms is still readily apparent in primates. Given that visual signals from the fovea are not required for many vision-dependent aspects of refractive development in monkeys,[28–30] this is not a surprising finding.

Because there were no systematic interocular differences in corneal power, anterior chamber depth or lens thickness, the strong correlation between interocular differences in vitreous chamber depth and the degree of anisometropia in the FF and NF monkeys shows that, as in form-deprived macaques,[18] lens-reared marmosets (Totonelly KC, et al. *IOVS* 2008;49:ARVO E-Abstract 3589), and lens-reared and form-deprived chicks,[4,5] the pattern of peripheral refraction is primarily determined by the shape of the posterior globe. Moreover, the changes in ocular shape and the pattern of peripheral refractive error in the FF defocus monkeys are similar to those observed in many humans. Specifically, monkeys with experimentally induced myopia and humans with naturally occurring myopia typically exhibit relatively prolate eyes and peripheral hyperopia.[14,19–23] On the other hand, the hyperopic fellow eyes of the FF defocus monkeys are more oblate and show relative peripheral myopia, as do many humans with emmetropia and hyperopia.[13,14,19]

As mentioned in the Introduction, the presence of peripheral hyperopia has been identified as a possible risk factor for myopia progression in humans,[25,26] and experimentally induced peripheral hyperopia has been shown to produce central axial myopia in monkeys.[30] However, the presence of relative peripheral hyperopia in monkeys with central myopia produced by full-field hyperopic defocus or form deprivation demonstrates that the association between central myopia and peripheral hyperopia is not necessarily causal. Because the optical consequences of imposed hyperopic defocus are likely to be more severe at the fovea and to decrease with eccentricity, it is reasonable to expect that experimentally imposed hyperopic defocus would result in a more prolate eye. However, given that form deprivation produces qualitatively similar changes, it seems more likely that some degree of peripheral hyperopia comes about as a result of constraints, presumably anatomic, that cause the eye to become less oblate and more prolate as it increases in central axial length. Nonetheless, it is reasonable to speculate that the changes in eye shape that are associated with central myopic axial elongation and the resultant changes in the pattern of peripheral refractive error put the eye at risk for additional myopia progression. Although correcting lenses can eliminate myopic defocus at the fovea, with most traditional correcting strategies much of the periphery will experience absolute hyperopic defocus (as illustrated in Fig. 9), which, as mentioned, is a strong stimulus for central axial elongation. Moreover, recent studies suggest that traditional negative-powered spectacle lenses actually exaggerate the amount of relative peripheral hyperopia in myopic eyes, which may further promote central axial elongation.[41,42] Thus, regardless of whether peripheral hyperopia plays a key role in the onset of central axial myopia, it may play a significant role in myopia progression commonly observed in patients with juvenile-onset myopia.

The fact that the effects of optical defocus, like form deprivation, are mediated by local-acting, vision-dependent mechanisms in primates has important implications for the role of

vision in the genesis of myopia and for the development of optical treatment strategies for controlling ocular growth. First, the presence of local growth-regulating mechanisms provides a way for peripheral vision to alter ocular shape and central axial length in a manner that is independent of central refractive error, which supports the hypothesis that peripheral vision, in particular peripheral hyperopic defocus, can promote the development and progression of myopia. However, because visual experience in the periphery can alter ocular shape and central axial length in a manner that is independent of the central refractive error, it should be possible to design optical correction strategies that allow clear, unrestricted central vision but simultaneously eliminate peripheral growth signals or produce peripheral visual signals that normally reduce or stop axial elongation. It is possible that lenses that increase curvature of field and reduce or eliminate relative peripheral hyperopia may decrease myopia progression.

Acknowledgments

The authors thank Hope Queener for assistance in developing software critical to the MRI experiments.

References

1. Wallman J, Winawer J. Homeostasis of eye growth and the question of myopia. *Neuron.* 2004;43:447–468.
2. Norton TT, Siegwart JT. Animal models of emmetropization: matching axial length to the focal plane. *J Am Optom Assoc.* 1995;66:405–414.
3. Hodos W, Kuenzel WJ. Retinal-image degradation produces ocular enlargement in chicks. *Invest Ophthalmol Vis Sci.* 1984;25:652–659.
4. Wallman J, Gottlieb MD, Rajaram V, Fugate-Wentzek L. Local retinal regions control local eye growth and myopia. *Science.* 1987; 237:73–77.
5. Diether S, Schaeffel F. Local changes in eye growth induced by imposed local refractive error despite active accommodation. *Vision Res.* 1997;37:659–668.
6. Smith III EL, Huang J, Hung L-F, et al. Hemiretinal form deprivation: evidence for local control of eye growth and refractive development in infant monkeys. *Invest Ophthalmol Vis Sci.* 2009;50: 5057–5069.
7. Bartmann M, Schaeffel F, Hagel G, Zrenner E. Constant light affects retinal dopamine levels and blocks deprivation myopia but not lens-induced refractive errors in chickens. *Vis Neurosci.* 1994;11: 199–208.
8. Kee C-S, Marzani D, Wallman J. Differences in time course and visual requirements of ocular responses to lenses and diffusers. *Invest Ophthalmol Vis Sci.* 2001;42:575–583.
9. Schaeffel F, Hagel G, Bartmann M, Kohler K, Zrenner E. 6-Hydroxydopamine does not affect lens-induced refractive errors but suppresses deprivation myopia. *Vision Res.* 1994;34:143–149.
10. Hodos W, Erichsen J. Lower-field myopia in birds: an adaptation that keeps the ground in focus. *Vision Res.* 1990;30:653–657.
11. Miles FA, Wallman J. Local ocular compensation for imposed local refractive error. *Vision Res.* 1990;30:339–349.
12. Ferree CE, Rand G. Interpretation of refractive conditions in the peripheral field of vision: a further study. *Arch Ophthalmol.* 1933; 9:925–938.
13. Ferree CE, Rand G, Hardy C. Refraction for the peripheral field of vision. *Arch Ophthalmol.* 1931;5:717–731.
14. Millodot M. Effect of ametropia on peripheral refraction. *Am J Optom Physiol Opt.* 1981;58:691–695.
15. Rempt R, Hoogerheide J, Hoogenboom WPH. Peripheral retinoscopy and the skiagram. *Ophthalmologica.* 1971;162:1–10.
16. Seidemann A, Schaeffel F, Guirao A, Lopez-Gil N, Artal P. Peripheral refractive error in myopic, emmetropic, and hyperopic young subjects. *J Opt Soc Am A.* 2002;19:2363–2373.
17. Atchison DA, Pritchard N, White SD, Griffiths AM. Influence of age on peripheral refraction. *Vison Res.* 2005;45:715–720.
18. Huang J, Hung L-F, Ramamirtham R, et al. Effects of form deprivation on peripheral refraction and ocular shape in infant rhesus monkeys (*Macaca mulatta*). *Invest Ophthalmol Vis Sci.* 2009;50: 4033–4044.
19. Mutti DO, Sholtz RI, Friedman NE, Zadnik K. Peripheral refraction and ocular shape in children. *Invest Ophthalmol Vis Sci.* 2000;41: 1022–1030.
20. Atchison DA, Pritchard N, Schmid KL. Peripheral refraction along the horizontal and vertical visual fields in myopia. *Vision Res.* 2006;46:1450–1458.
21. Atchison DA, Jones CE, Schmid KL, et al. Eye shape in emmetropia and myopia. *Invest Ophthalmol Vis Sci.* 2004;45:3380–3386.
22. Atchison DA, Pritchard N, Schmid KL, Scott DH, Jones CE, Pope JM. Shape of the retinal surface in emmetropia and myopia. *Invest Ophthalmol Vis Sci.* 2005;46:2698–2707.
23. Logan NS, Gilmartin B, Wildsoet CF, Dunne MCM. Posterior retinal contour in adult human anisomyopia. *Invest Ophthalmol Vis Sci.* 2004;45:2152–2162.
24. Stone RA, Flitcroft DI. Ocular shape and myopia. *Ann Acad Med Singapore.* 2004;33:7–15.
25. Hoogerheide J, Rempt F, Hoogenboom WP. Acquired myopia in young pilots. *Ophthalmologica.* 1971;163:209–215.
26. Mutti DO, Hayes JR, Mitchell GL, et al. Refractive error, axial length, and relative peripheral refractive error before and after the onset of myopia. *Invest Ophthalmol Vis Sci.* 2007;48:2510–2519.
27. Schmid G. Retinal steepness vs. myopic shift in children. *Optom Vis Sci.* 2004;12S:23.
28. Smith EL III, Kee C-S, Ramamirtham R, Qiao-Grider Y, Hung LF. Peripheral vision can influence eye growth and refractive development in infant monkeys. *Invest Ophthalmol Vis Sci*. 2005;46: 3965–3972.
29. Smith EL III, Ramamirtham R, Qiao-Grider Y, et al. Effects of foveal ablation on emmetropization and form-deprivation myopia. *Invest Ophthalmol Vis Sci.* 2007;48:3914–3922.
30. Smith EL III, Hung LF, Huang J. Relative peripheral hyperopic defocus alters central refractive development in monkeys. *Vision Res.* 2009;49:2386–2392.
31. Smith EL III, Hung LF. The role of optical defocus in regulating refractive development in infant monkeys. *Vision Res*. 1999;39: 1415–1435.
32. Hung L-F, Ramamirtham R, Huang J, Qiao-Grider Y, Smith EL III. Peripheral refraction in normal infant rhesus monkeys. *Invest Ophthalmol Vis Sci.* 2008;49:3747–3757.
33. Harris WF. Algebra of sphero-cylinders and refractive errors, and their means, variance, and standard deviation. *Am J Optom Physiol Opt.* 1988;65:794–902.
34. Keselman HJ, Algina J, Kowalchuk RK. The analysis of repeated measures designs: a review. *Br J Math Stat Psy.* 2001;54:1–20.
35. Kee C-S, Hung LF, Qiao-Grider Y, et al. Temporal constraints on experimental emmetropization in infant monkeys. *Invest Ophthalmol Vis Sci.* 2007;48:957–962.
36. Raviola E, Wiesel TN. An animal model of myopia. *N Engl J Med.* 1985;312:1609–1615.
37. Troilo D, Totonelly KC. Studies of eye shape and peripheral refractive state in marmosets reared with single vision contract lenses. Presented at: 12th International Myopia Conference; July 8–12, 2008; Palm Cove, Australia.
38. Quick MW, Boothe RG. A photographic technique for measuring horizontal and vertical eye alignment throughout the field of gaze. *Invest Ophthalmol Vis Sci.* 1992;33:234–246.
39. Rodieck RW. *The First Steps in Seeing*. Sunderland, Massachusetts: Sinauer Associates, Inc.; 1998
40. Norton TT, Siegwart JT. Local myopia produced by partial visual-field deprivation in tree shrew. *Soc Neurosci Abstr.* 1991;17:558.
41. Tabernero J, Vazquez D, Seidemann A, Uttenweiler D, Schaeffel F. Effects of myopic spectacle correction and radial refractive gradient spectacles on peripheral refraction. *Vision Res.* 2009;49:2176–2186.
42. Lin Z, Martinez A, Chen X, et al. Peripheral defocus with single-vision spectacle lenses in myopic children. *Optom Vis Sci*. 2010; 87:4–9.